Taiwania 68(1): 8–22, 2023
DOI: 10.6165/tai.2023.68.8

A statistical method to generate high-resolution climate datasets for modeling plant distribution range and range shifts under climate change in mountainous areas

Chi-Cheng LIAO[1,*] Huan-Yu LIN[2,3], Su-Wei FAN[2]

1. Department of Life Science, Chinese Culture University, Taiwan, R.O.C. *2.* Taiwan Forestry Research Institute, Taipei, Taiwan. *3.* Department of Forestry and Natural Resources, National Ilan University, Yilan County, Taiwan. *Corresponding author's email: hunter_yyl@yahoo.com.tw; Tel: +886-2-2861-0511 ext. 26233; Fax: +886-2-2861-7507

(Manuscript received 20 September 2022; Accepted 29 November 2022; Online published 2 January 2023)

ABSTRACT: This study aims to develop a statistical method to generate high-resolution historical and future climate datasets for modeling plant distributions in mountainous area. Two climate datasets that were from Taiwan Climate Change Projection Information and Adaptation Knowledge Platform (TCCIP) and meteorological stations were used to construct two historical climate datasets with 50 × 50 m^2 spatial resolution, respectively. The two historical climate datasets presented similar temperature pattern but distinct precipitation patterns in northern Taiwan (NTWN). Random Forests (RF) had predicted similar distribution range of natural grassland along mountain ridge when RF were applied by the two climate datasets, whereas RF had predicted restricted distribution range when it was applied by true absence data. The two historical climate datasets were added to the relative changes of climate variables representing four future climate scenarios. RF method based on the future climate datasets predicted habitat loss of natural grassland at the mid and end of this century, regardless of climate datasets and four warming scenarios. Due to the altitudinal limits of NTWN, there is almost no chance for natural grassland to track their climatic requirements toward higher elevations under climate change. High-resolution historical and future climate datasets generated by the statistical method were useful for species distribution model to project species potential distribution range in mountainous area and were available to examine species range shifts under climate change. Model performances based on the high-resolution climate dataset may have better expressed the climatic requirements and exact climatic niches of species in mountainous areas.

KEY WORDS: Climate change, high-resolution climate dataset, Random Forests, species distribution model, Taiwan.

INTRODUCTION

Climate change has been recognized as one of the major forces threatening biodiversity and impacting natural ecosystems on a global scale (Keppel *et al*., 2012; Miles *et al*., 2004; Orsenigo *et al*., 2018; Thomas *et al*., 2004; Walther, 2010). Climate change could fundamentally alter the species compositions, forest structures, and species distribution patterns (Allen *et al*., 2010; Hamann and Wang, 2006). Mountain species is particularly susceptible to climate change, they will shift distribution range along mountain slopes to track climatic requirements in response to climate change (Fatemi *et al*., 2018; Vanneste *et al*., 2017; Zhao *et al*., 2016). However, mountainous areas are characterized by steep climatic gradients and support patchy habitats that had caused restriction and fragmentation of species distribution ranges along mountain slopes (Dobrowski, 2011; Lannuzel *et al*., 2021). Due to the steep climatic gradients and patchy habitats, it is a crucial task to identify species distribution range in mountainous areas and it is more difficult to evaluate species range shifts under climate change in mountainous areas with complex topography.

Species distribution models (SDMs) are powerful tools for ecologists to project species potential distribution range and to predict species range shifts under climate change. During the last decade, high-resolution climate datasets had been generated from various data sources in order to improve the performances of SDMs in mountainous areas. These climate data sources include global climate dataset (Godsoe *et al*., 2015; Lin *et al*., 2018; Maria and Udo, 2017; Mohapatra *et al*., 2019; Schorr *et al*., 2012; Wang *et al*., 2016; Zhu *et al*., 2018), climate data from dataloggers (Ashcroft and Gollan, 2012; Ashcroft *et al*., 2012; Dingman *et al*., 2013; Fridley, 2009; Greiser *et al*., 2018; Vanwalleghem and Meentemeyer, 2009) or meteorological stations (Liao and Chen, 2021; Meineri and Hylander, 2017). High-resolution climate dataset had been successfully interpolated from meteorological stations in previous studies and had accurately captured climate heterogeneity of mountainous areas in a subtropical island (Liao and Chen, 2021, 2022). Alternatively, local gridded climate dataset had been used as a data source to interpolate high-resolution climate dataset in the same island (Lin *et al*., 2018; Lin *et al*., 2020). Local gridded climate dataset that was used as data source in the Lin *et al*. (2018) was downscaled from AR5 General Circulation Models (GCMs). The working group of Taiwan Climate Change Projection Information and Adaptation Knowledge Platform (TCCIP) had generated 5 × 5 km^2 gridded climate dataset from GCMs to represent historical climates and future scenarios of Taiwan island (Lin *et al*., 2022). High-resolution climate datasets derived from either meteorological stations (Liao and Chen, 2021,

2022) or TCCIP's 5 × 5 km^2 gridded climate dataset (Lin *et al*., 2018; Lin *et al*., 2020) had been applied for SDMs to predict the historical distribution range of plant species in mountainous areas. It is crucial to examine the differences in model results when SDMs were applied by these two types of high-resolution climate datasets.

Additionally, SDMs are also powerful tools to evaluate species range shifts in response to climate change (Mohapatra *et al*., 2019; Xu *et al*., 2021; Zhu *et al*., 2018). High-resolution future climate projection was necessary for SDMs to accurately project species range shifts in response to climate change. For Taiwan island, TCCIP provides 5 × 5 km^2 gridded climate dataset representing future climate projections (Lin *et al*., 2022). The TCCIP's future climate projections presents relative changes of climate variables in comparison with the baseline period (1960-2012). In this study, a statistical method was developed to generate high-resolution future climate projections by downscaling TCCIP's future climate projections. There are two datasets generated in this study representing historical climate conditions, the one was derived from meteorological data and the other from the TCCIP's 5 × 5 km^2 gridded climate dataset. The two historical climate datasets were separately added the relative changes of TCCIP's future climate projections. The historical climate datasets and future scenarios were both applied for SDMs to predict the current species distributions and to evaluate species range shifts in response to climate change.

Random Forest (RF) is a powerful machine learning classifier to provide accurate predictions of species distributions (Boulesteix *et al*., 2012; Breiman, 2001; Liaw and Wiener, 2002). RF has become a popular method to identify correlation between geographical extent and climate factors of species (Evans and Cushman, 2009; Hu *et al*., 2017; Iturbide *et al*., 2018; Mi *et al*., 2017; Mohapatra *et al*., 2019; Williams *et al*., 2009). A previous study had evidently demonstrated a better performance of RF than the other five models on predicting potential distribution range of natural grassland in mountainous area (Liao and Chen, 2022). RF was performed in this study to project historical distribution range of natural grassland and to evaluate its range shifts in response to climate change in mountainous area.

In this study, natural grassland was selected as the target vegetation of SDMs predictions. Natural grassland is a prominent and long-term persistent vegetation type in mountainous areas with the elevations lower than 1,000 m above sea level (asl.) in northern Taiwan (NTWN) (Li *et al*., 2013; Liao *et al*., 2014). *Miscanthus sinensis* and *Pseudosasa usawai* are mostly the predominant species of natural grassland in NTWN (Liao *et al*., 2012; Liao *et al*., 2014). The occurrences of natural grassland along mountain ridge was evidently determined by multiple climate factors, such as relatively heavy precipitation and strong winds in NTWN (Liao and Chen, 2022). The climate condition of natural grassland at low elevations in NTWN was significantly different from that of natural grassland at subtropical high mountain (Korner, 1998; Korner and Paulsen, 2004).

The major objective of this study aims to develop a statistical method to generate historical and future climate datasets for modeling plant distributions in mountainous areas. Based on the statistical method, two historical climate datasets with 50 × 50 m^2 spatial resolution were derived from meteorological stations and TCCIP's gridded climate dataset, respectively. The two historical climate datasets were both applied with RF to project potential distribution range of natural grassland. It is hypothesized that high-resolution climate dataset derived from meteorological stations will result in more accurate model predictions than that derived from GCM's gridded climate dataset, such as TCCIP. Future climate datasets representing warming scenarios generated by the statistical method were also applied for the RF to examine range shifts of natural grassland under climate change.

MATERIALS AND METHODS

Study area

Taiwan is a subtropical island (21°55'- 25°20'N, 119°30'- 122°00'E) located at the western edge of the Pacific Ocean, 150 km to the southeast coast of Mainland China (Fig. 1). The subtropical island is characterized by monsoon climate (Chen and Tsai, 1983; Su, 1984). Southwest monsoon prevails less than 4 months in summer which conveys moisture to the southern and western slopes of the island's Central Mountain Range. On the other hand, northeast monsoon in winter prevails 6 months per year in Taiwan which brings heavy rainfall and strong winds in northern and eastern slopes of the Central Mountain Range. Northeast monsoon had significant effects on the plant species distribution in Taiwan (Chiou *et al*., 2010). Particularly, northeast monsoon associated with typhoon brings extremely high rainfall in the northern Taiwan (NTWN) (Liao and Chen, 2022) that caused a steep precipitation gradient from the coast to inland areas of NTWN. The annual precipitation decreased from more than 6,000 mm at the northeastern slope to 1,900 mm at the southwestern slope of the mountain ridge. The mean monthly temperatures at mountain ridge range from 11.3 °C in winter to 20.5 °C in summer and that at coastal area from 17.9 °C in winter to 26.6 °C in summer (Liao and Chen, 2022).

The study area ranges from 24°57' to 25°17'N and 121°24' to 122°00'E in NTWN (Fig. 1) and the area is about 1,031 square kilometers (103,100 hectares). The highest mountain peak, Qixingshan, in the study area is 1,120 m above sea level (asl.). Evergreen broad-leaved forest is the major vegetation type in NTWN (Hsieh *et al*., 1997; Li *et al*., 2013; Liao *et al*., 2012). There is no deciduous forest in NTWN and native deciduous tree

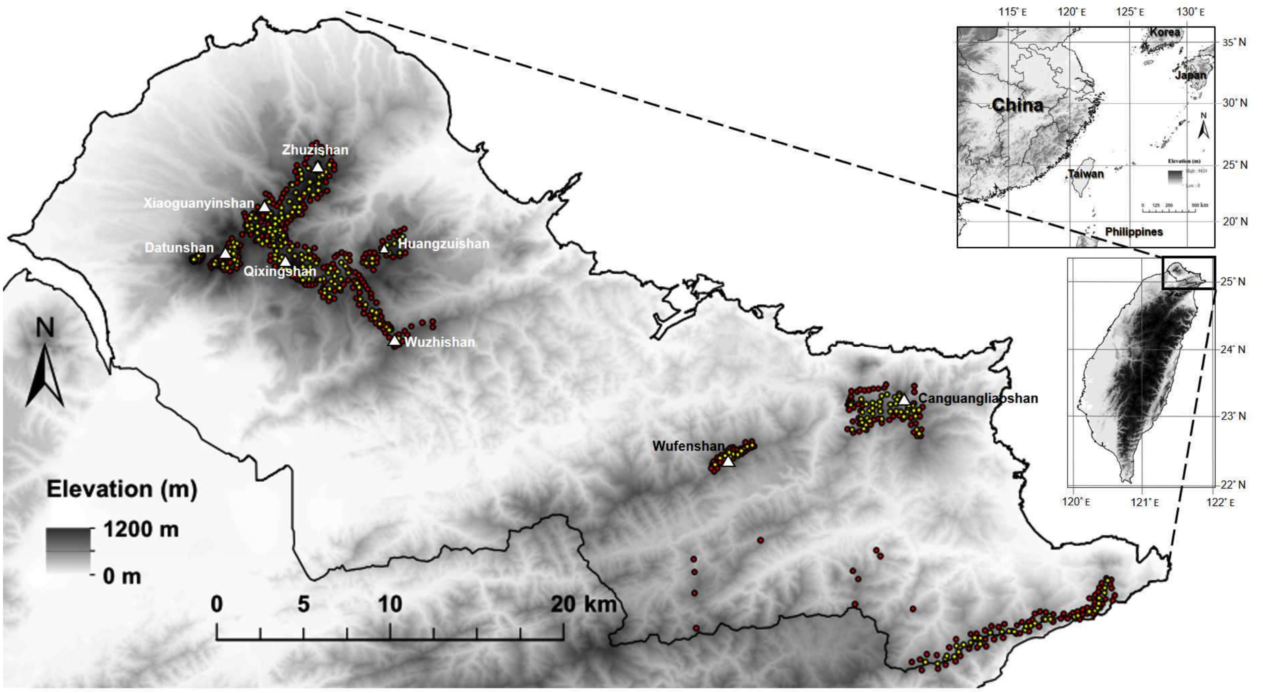

Fig. 1. Maps show the study area in northern Taiwan and the geographical location of Taiwan and neighboring countries (upper right map). Presence and absence of grassland in northern Taiwan presented by yellow and red solid dots, respectively. Mountain tops were represented by white triangles.

species scattered in the native forests of NTWN. The forests in NTWN are dominated by species of *Castanopsis*, *Cleyera*, *Cyclobalanopsis*, *Dendropanax*, *Elaeocarpus*, *Engelhardia*, *Gordonia*, *Helicia*, *Ilex*, *Keteleeria*, *Limlia*, *Litsea*, *Machilus*, *Meliosma*, *Michelia*, *Pinus*, *Schefflera*, *Symplocos*, and *Trochodendron* with a mean canopy height of 10 m (Li *et al*., 2013). Natural grassland is the target vegetation of this study and it was frequently observed at mountain ridge from coast to inland areas in NTWN (Fig 1).

Vegetation data collection

Distribution of natural grassland was constantly along the mountain ridge, whereas elevation ranges vary along different mountain ridges in the study area (Fig. 1). The elevation ranges of the natural grassland at the southeast border of the study area extents from 280 to 600 m asl. and that along the mountain ridge from Wufenshan to Canguangliaoshan and from Datunshan to Zhuzishan extent from 360 to 737 m asl. and from 780 to 1070 m asl., respectively. Presence and absence data of natural grassland were collected along the roads and mountain trails in NTWN. Field investigation had observed abrupt transitions from natural grassland at mountain ridge to closed-canopy forests along mountain slopes in NTWN. Thus, the presence data of natural grassland were defined as the vegetation without shrubs or trees, whereas the closed-canopy forests were defined as absence data. Field investigation had recorded 252 presence and 372 absence points for modeling the potential range of natural grassland (Fig. 1).

The study area is divided into 50×50 m^2 gridded cells and duplicated records of the presence data were spatially verified to ensure only one occurrence within each gridded cell. Two types of absence data were used in this study. The 372 absence points recorded in the field investigation were true absence data. True absence data had practically delineated geographical boundaries and characterized the climate environments of natural grassland (Liao and Chen, 2022). Meanwhile, pseudo-absence data was random points selected from the gridded cells within the study area. Pseudo-absence data, known as background data, represented the available environmental conditions of the study area. Presence and true/pseudo-absence data of natural grassland were used to construct the training datasets of species distribution model. On the contrary, grasslands close to the farmland which pronouncedly caused by anthropogenic disturbances were not target vegetation in this study.

Downscale of climate dataset

The TCCIP is a climate research project with the most predominant climate data provider and national adaptation policy maker in Taiwan (Lin *et al*., 2022). The TCCIP provided a gridded climate surface with 5×5 km^2 spatial resolution (Fig. 2A). Time period of the TCCIP climate dataset spans from 1960 to 2012 (Weng and Yang, 2012). Spatial resolution of 5×5 km^2 was not available to present the climate heterogeneity in the mountainous areas (Lin *et al*., 2018). In this study, the TCCIP climate

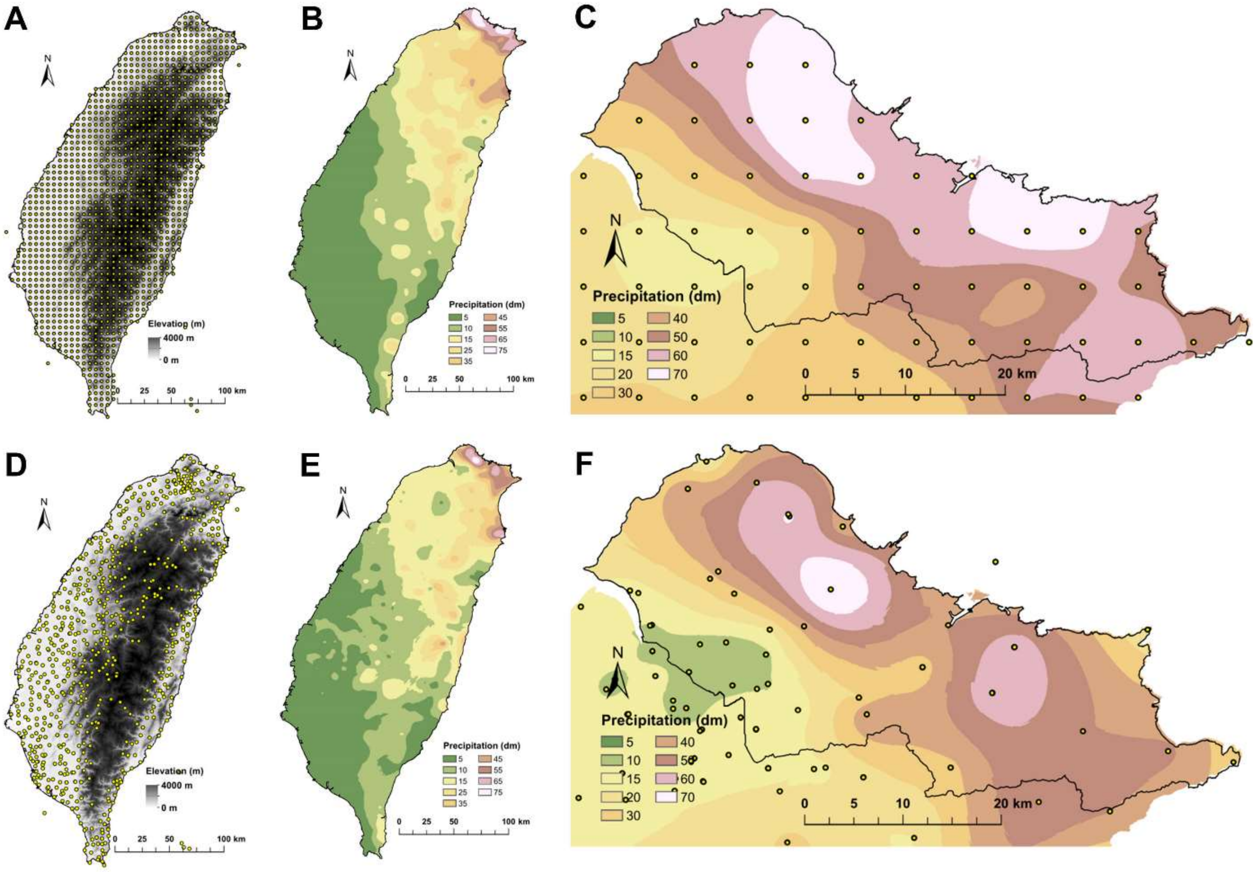

Fig. 2. The TCCIP's gridded climate dataset and climate surface derived from TCCIP at the upper three maps (**A**, **B**, and **C**) and the 463 meteorological stations and climate surface derived from meteorological data at lower three maps (**D**, **E**, and **F**). The left maps present gridded cells of TCCIP with 5 × 5 km^2 spatial resolution (**A**) and locations of 463 meteorological stations (**D**) in Taiwan. The two central maps are climate surfaces represented precipitation of January in Taiwan island that were derived from TCCIP (**B**) and meteorological stations (**E**), respectively. The right two maps were zoomed in to the northern Taiwan (**C** and **F**). TCCIP is the Taiwan Climate Change Projection Information and Adaptation Knowledge Platform.

dataset was downscaled to generate gridded climate dataset with 50 × 50 m^2 spatial resolution to capture steep environmental features along mountain slopes. The downscaling procedures of the historical climate dataset includes: (1) interpolation of TCCIP climate dataset to generate smooth surfaces of climate variables; (2) generation of gridded cells with 50 × 50 m^2 spatial resolution to extract TCCIP climate data; (3) altitudinal adjustment of the extracted climate data.

In order to make comparable the TCCIP climate data with the meteorological data, the TCCIP's historical climate dataset with the time period from 2000 to 2012 was retrieved from the original TCCIP climate dataset (1960-2012). The retrieved TCCIP climate dataset (2000-2012) was used to interpolate smooth surfaces of climate variables by means of Kriging method to present climate characteristics of Taiwan island (Fig. 2B and 2C). The interpolations were performed in ArcInfo software (ESRI, Redlands, California, USA) and had generated .tif files of climate variables. Gridded cells with spatial resolution of 50 × 50 m^2 were also generated in ArcInfo software. A total of more than 0.4 million gridded cells were generated in the study area. For each gridded cell, longitude, latitude, and elevation were obtained from a digital terrain model (DTM) with a resolution of 20 by 20 meters been developed by the Department of Geography, Chinese Culture University. The elevation data obtained from DTM was named as DElev. Subsequently, the 50 × 50 m^2 gridded cells were mapped and overlapped with the .tif files of the TCCIP climate surfaces to extract climate data. The TCCIP climate dataset with 50 × 50 m^2 spatial resolution was named as TCD50. Furthermore, elevations of the TCCIP points were also interpolated by Kriging method in ArcInfo software to generate a smooth elevation surface (TElev). The gridded cells of TCD50 was overlapped with TElev to extract the elevation data. The differences between DElev and TElev was used for altitudinal adjustment of TCD50. The function for altitudinal adjustment is: AdjTCD50 = slope × (DElev – TElev) + TCD50. The abbreviation AdjTCD50 is adjusted TCCIP climate data with 50 × 50 m^2 spatial resolution. The slope of the function, namely the empirical lapse rate, was

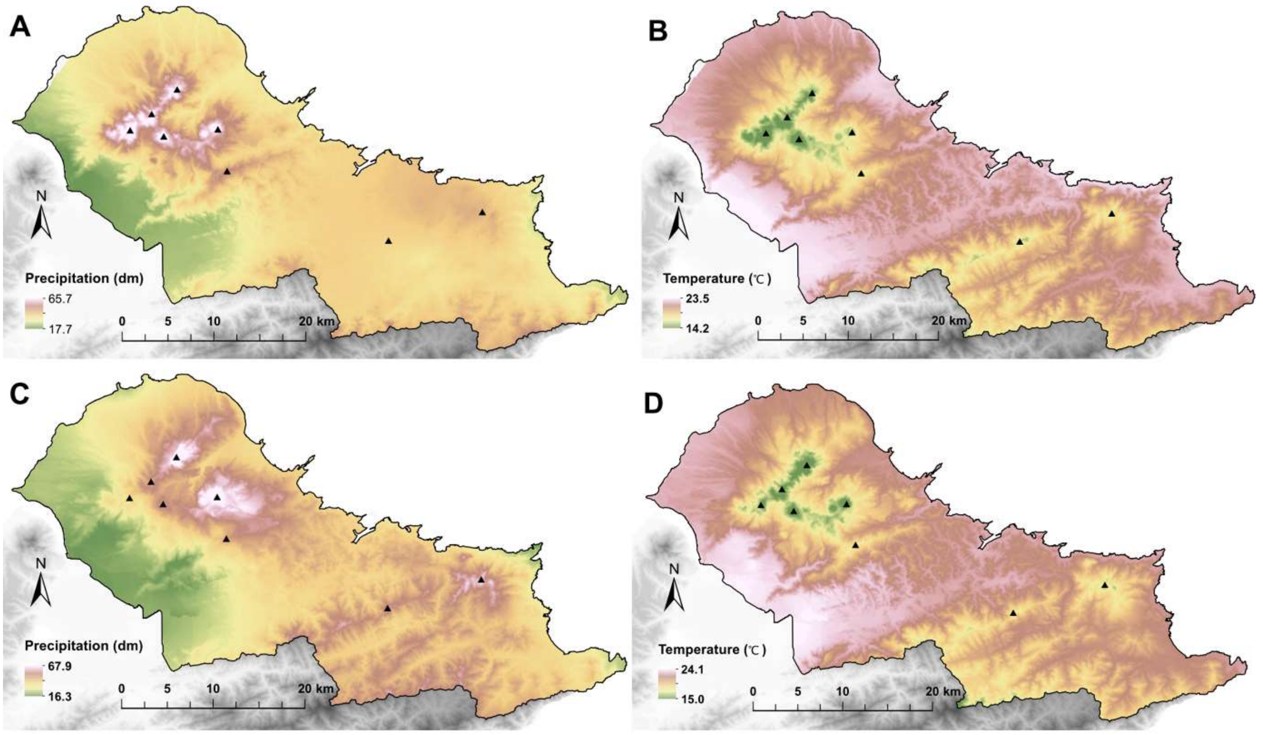

Fig. 3. Climate surfaces with 50 × 50 m^2 spatial resolution derived from TCCIP climate dataset (**A** and **B**) and meteorological data (**C** and **D**). The maps present the annual total precipitation (left column) and annual mean temperature (right column) after altitudinal adjustment. The precipitation pattern derived from TCCIP climate dataset presents highest precipitation along mountain ridge in northern Taiwan (NTWN) (**A**). On the contrary, climate surface derived from the meteorological data presents the highest precipitation at the northeastern slope of the mountain ridge and significant topographical heterogeneity of precipitation at eastern area of NTWN (**C**). The temperature patterns were slightly different along mountain ridge between the right two maps (**B** and **D**). Mountain tops represented by dark triangle were the same as in Fig. 1. TCCIP is the Taiwan Climate Change Projection Information and Adaptation Knowledge Platform.

the slope of linear correlation calculated from the elevation and climate data of the nearest 16 TCCIP points. Linear regression model was implemented by "stats" package within the R environment (Chambers and Hastie, 1992).

In addition to the AdjTCD50, another climate dataset was derived from the meteorological data (Fig. 2D) The daily data of meteorological stations from 2000 to 2012 was downloaded from the website of Central Weather Bureau (CWB, https://www.cwb.gov.tw/V7/forecast/) and were used to calculate mean monthly temperature and precipitation. Mean monthly temperature and precipitation derived from meteorological stations were imported to ArcInfo software to generate smooth surfaces of climate variables (Fig. 2E and 2F) by means of Kriging method. The .tif files of smooth climate surfaces derived from meteorological data were also overlapped with the 50 × 50 m^2 gridded cells to extract climate data. This is the meteorological climate dataset with 50 × 50 m^2 spatial resolution (MCD50). For each gridded cell, the same function was used to adjust MCD50 and the function is: AdjMCD50 = slope × (DElev – TElev) + MCD50. The abbreviation AdjMCD50 is adjusted meteorological climate data with 50 × 50 m^2 spatial resolution. It is noteworthy that the slope of this function was calculated from the nearest 12 meteorological stations.

The altitudinal adjusted climate data, including AdjTCD50 and AdjMCD50, were used as historical climate datasets for modeling species distributions. The two climate datasets were both created taking into account the following 9 variables: mean annual temperature (Tann), mean maximum temperature of the warmest month (Twrm), mean minimum temperature of the coldest month (Tcld), mean temperature in summer (Tsmr) and winter (Twnt), temperature differences between warmest and coldest months (Tdif), annual total precipitation (Pann), total precipitation in summer (Psmr) and winter (Pwnt). The climate surfaces derived from TCCIP and meteorological data presented distinct precipitation patterns (Pann) and similar temperature pattern (Tann) in the NTWN (Fig. 3).

Downscale of future climate projection

The TCCIP also provided future climate projections based on different AR5 General Circulation Models (GCMs) and four scenarios (Weng and Yang, 2012). The future climate projections of Taiwan island were downscaled from 49 GCMs during the 5th phase of the

Coupled Model Intercomparison Project (CMIP5) and covers three time periods (2016-2035, 2046-2065, 2081-2100) and four Representative Concentration Pathways (RCPs) (Lin *et al.*, 2018; Weng and Yang, 2012). The four RCPs have been used to indicate various warming conditions in the future from the highest emission and the warmest scenario (RCP 8.5), to two intermediate emissions and scenarios (RCP 6.0, RCP 4.5), to the lowest emission and the most mitigated scenario (RCP 2.6) (IPCC, 2013). Among the 49 available GCMs, only the Community Earth System Model, version 1, with the Community Atmosphere Model, version 5 (CESM1-CAM5) was used in this study. The CESM1-CAM5 which consists of coupled atmosphere, ocean, land and sea ice component models is an open source, comprehensive model used in simulations of the Earth's past, present and future climates (Kay *et al.*, 2015). The future climate projection of Taiwan island was downscaled into 5 × 5 km^2 gridded climate dataset by TCCIP based on the CESM1-CAM5 climate model.

The TCCIP gridded future climate projections presented the relative changes of the mid and late of the century to the baseline climate data 1960-2012, whereas the time period of AdjTCD50 and AdjMCD50 generated in this study was the early of this century 2000-2012. Thus, the time period of baseline climate data should be revised from the late of the 20th century (1960-2012) to the early of the 21th century (2000-2012). The future climate projection presented by relative changes between the early (2000-2012) and mid as well as between early and late of the 21th century were necessary to recalculate. The relative changes between the early and mid of the 21th century was obtained by multiplying the relative changes of TCCIP future climate projections by the ratio of the year time length between the early and mid of 21th century to the year time length between baseline (1960-2012) and mid of the 21th century. The relative changes between the early and late of the 21th century was also calculated by the same method.

The relative changes between early and mid as well as between early and late of the 21th century were also 5 × 5 km^2 gridded data that were used to generate .tif files of smooth climate surfaces by means of Kriging method performed in ArcInfo software. The gridded cells with 50 × 50 m^2 spatial resolution was overlapped with the .tif files of smooth climate surfaces to extract the relative changes of climate data. The two historical climate datasets, AdjTCD50 and AdjMCD50, were separately overlapped with the relative changes of 50 × 50 m^2 gridded climate datasets to project future climates (Supplement: Fig. S1 and S2).

Modelling technique

In this study, Random Forests (RF) implemented by "biomod2" package in R software (Thuiller *et al.*, 2016) was used to project potential distribution range of natural grassland and to predict future changes under different climate scenarios. Although "biomod2" provides several model algorithms in the package, performance of RF was evidently much better than the other models (Liao and Chen, 2022). RF is a machine learning method that handles numerous variables and is capable of detecting complex relationships among model variables without making a prior assumption about the type of relationship (Breiman, 2001). The two gridded climate datasets, AdjTCD50 and AdjMCD50, were used as two testing datasets to evaluate the potential distribution range of natural grassland. The two training datasets were generated from the overlapping of presence and true/pseudo-absence data of natural grassland with AdjTCD50 and AdjMCD50 to extract climate data. Presence and true/pseudo-absence data of natural grassland with climate data were randomly re-sampled 200 data records to create training datasets. The training datasets were divided into two subsets in order to evaluate model accuracy. The first was 80% random subset of the presence and absence data to train the model, while the remaining 20% was used for evaluation. The 80% and 20% random subsets were resampled 100 times to quantify the uncertainties in model predictions. Model results can be mapped and overlapped with the presence points of natural grassland to detect the model performance (Liao and Chen, 2022). Field investigation had verified distinct boundaries between natural grassland and evergreen broadleaved forests and, therefore, a better model performance can be determined by a considerable overlap between model results and presence points of natural grassland. In addition, model accuracy was represented by True Skill Statistics (TSS) and receiver operating characteristic (ROC) curve (Fois *et al.*, 2015; Lannuzel *et al.*, 2021; Qiao *et al.*, 2019; Thuiller *et al.*, 2016; Xu *et al.*, 2021).

RESULTS

Historical distribution ranges

Historical distribution range predicted by RF based on the two climate datasets presented similar distribution pattern of natural grassland along mountain ridge in NTWN (Fig. 4). Model results based on the presence and pseudo-absence data had wider distribution range along mountain ridge (Fig. 4A and 4C). No significant difference could be observed when RF method was applied by different climate datasets (Fig. 4A and 4C). However, it is evident that true absence data had profoundly restricted distribution range of natural grassland (Fig. 4b and 4d) in contrast to the model results based on the pseudo-absence data (Fig. 4A and 4C). Climate dataset had weak effects on shifting projection range of natural grassland, while true absence data had significant effects on restricting potential distribution range of natural grassland.

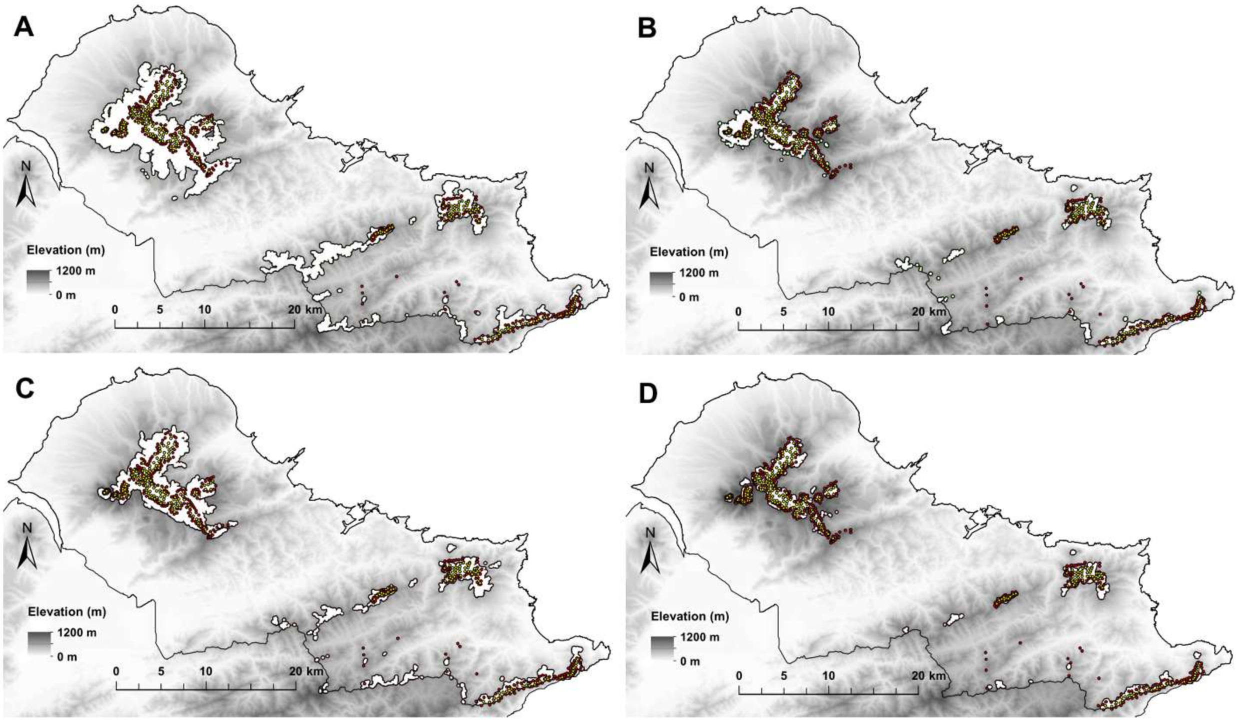

Fig. 4. Potential distribution range predicted by Random Forests (RF) based on the climate datasets with 50 × 50 m^2 spatial resolution derived from the TCCIP climate dataset (**A** and **B**) and meteorological data (**C** and **D**). The yellow and red circle with dark outline are presence and true absence points of natural grassland, respectively. White areas with dark outline are the potential distribution range predicted by Random Forests. Wider distribution ranges were presented based on presence and pseudo-absence data (**A** and **C**), whereas narrower distribution ranges were showed based on presence and true absence data (**B** and **D**). TCCIP is the Taiwan Climate Change Projection Information and Adaptation Knowledge Platform.

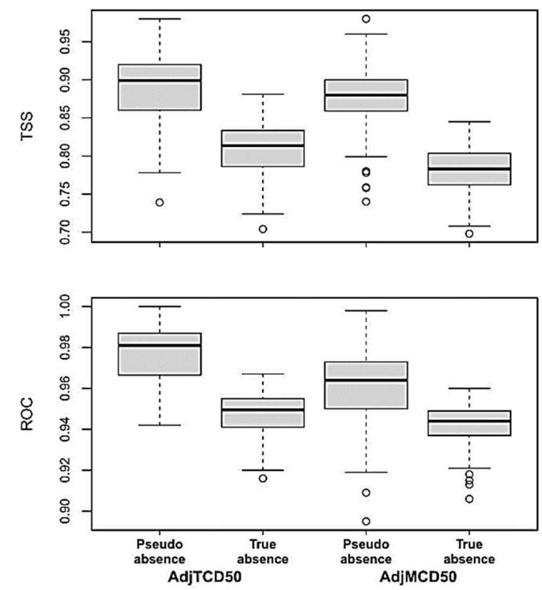

Fig. 5. Model evaluation indices, True Skill Statistics (TSS) and receiver operating characteristics (ROC) curve, of Random Forests (RF). The TSS and ROC value based on the adjusted TCCIP climate dataset with 50 × 50 m^2 spatial resolution (AdjTCD50) and adjusted meteorological climate dataset with 50 × 50 m^2 spatial resolution (AdjMCD50). The values of TSS and ROC were lower if the RF were implicated by true absence data. TCCIP is the Taiwan Climate Change Projection Information and Adaptation Knowledge Platform.

Model predictive accuracy represented by TSS and ROC presented inconsistent results. True absence data accurately restricted distribution range of natural grassland along mountain ridge, whereas the values of TSS and ROC were always lower when model was applied by true absence data, regardless of climate datasets (Fig. 5). Potential distribution range restricted by true absence data undoubtedly leads to a better model performance, since true absence data were locations of evergreen broadleaved forests and were geographically close to the boundaries of natural grassland. True absence data defines the geographical boundaries as well as climatic boundaries between natural grassland and evergreen broadleaved forests in NTWN. Gridded cells located at the border of natural grassland with similar climatic conditions were classified as either presence or absence cells that had significantly increased the omission and commission errors of model predictions. Under such circumstances, lower values of model evaluation indices (TSS and ROC), as a consequence of model prediction based on true absence data, did not lead to less accurate model performances. It is believed that true absence data associated with high-resolution climate datasets had resulted in good model performances and accurate distribution maps of plants.

Climate variables contributed most to the model predictions

Table 1. Importance of variables generated by Random Forest based on the true and pseudo-absence. Two climate datasets had been applied for the model predictions.

		AdjTCD50*		AdjMCD50#	
		Pseudo absence	True absence	Pseudo absence	True absence
Tmean	Mean annual temperature	1.5 ± 0.5	9.1 ± 1.7	9.2 ± 3.7	15.8 ± 3.1
Tsmr	Mean temperature in summer	7.2 ± 2.6	18.4 ± 3.3	21.1 ± 6.2	8.8 ± 1.8
Twnt	Mean temperature in winter	0.7 ± 0.2	9.3 ± 1.6	6.5 ± 3.3	12.0 ± 2.0
Twrm	Temperature in warmest month	18.2 ± 6.2	8.4 ± 1.2	45.0 ± 7.2	7.6 ± 1.3
Tcld	Temperature in coldest month	1.6 ± 0.6	9.2 ± 1.2	1.2 ± 0.4	6.5 ± 1.4
Tdif	Temperature differences between warmest and coldest months	15.4 ± 4.0	10.4 ± 1.3	3.2 ± 1.7	3.6 ± 0.6
Pann	Annual total Precipitation	7.7 ± 2.0	11.7 ± 1.7	1.4 ± 0.5	6.4 ± 0.8
Psmr	Precipitation in summer	18.6 ± 4.9	16.2 ± 1.7	7.3 ± 2.2	29.4 ± 2.5
Pwnt	Precipitation in winter	29.0 ± 6.2	7.2 ± 1.1	5.1 ± 1.4	10.0 ± 1.3

AdjTCD50*: adjusted TCCIP climate dataset with 50 × 50 m^2 spatial resolution. TCCIP is the Taiwan Climate Change Projection and Information Platform. AdjMCD50#: adjusted meteorological climate dataset with 50 × 50 m^2 spatial resolution.

were inconsistent between the two climate datasets or between two types of absence data (Table 1). Three climate variables, Pann, Twnt, and Tcld, have consistently low contributions to the model predictions. No specific climate variable had constantly high contribution to the model predictions.

Climate conditions of natural grassland

Frequency of gridded cells along gradients of climate variables demonstrated the climate conditions of NTWN. For most of the climate variables, slightly differences could be observed between the two climate datasets, AdjTCD50 and AdjMCD50 (Fig. 6). Only two climate variables, Twrm and Tcld, presented considerable differences between the two climate datasets (Fig. 6). The upper limits of Tcld and range of Twrm were significantly different between the two climate datasets. Among these two climate variables, Twrm contributed most to the model result when the model was applied by AdjMCD50 and pseudo-absence data (Table 1). The differences of these two climate variables resulted in a distinction of the Tdif between the two climate datasets. Temperature range, upper and lower limits of the Tdif were significantly different between the AdjTCD50 and AdjMCD50. However, there was no evidence to show the correlation between gradient length and ranges of climate variables (Fig. 6) and its contribution to model predictions (Table 1).

Along the gradient of the same climate variable, occurrences of natural grassland show no conspicuously different patterns between the two climate datasets (Fig. 6). The mechanism behind the contribution of climate variables to the model predictions is still elusive. It is simply concluded that occurrences of natural grassland along mountain ridge in NTWN was determined by multiple climate factors.

Future distribution range

The predicted suitable range of natural grassland under historical climate conditions (2000-2012) were mainly along mountain ridge in NTWN. Based on the four RCPs, RF method projected habitat loss of natural grassland at the mid and end of the 21th century (Fig. 7). Future climate change leads to a geographical constraint of natural grassland in NTWN. Due to the altitudinal limits in NTWN, there is almost no chance for natural grassland to shift their distribution range upslope to track the suitable climate requirements under climate change. Low elevation in NTWN is evidently resulted in a range restriction of natural grassland in the future.

The western area of NTWN was partly protected by Yanminghsan National Park. Anthropogenic disturbance has low effects on the distribution range of natural grassland in National Park. Thus, the major factor leads to the habitat loss of natural grassland is certainly the climate change at the mid and end of this century.

DISSCUSSION

Climate heterogeneity in mountainous areas was drastically induced by local ecological forces (Ashcroft *et al*., 2012; Dobrowski, 2011; Lenoir *et al*., 2017; Meineri and Hylander, 2017) and it can be difficult to distinguish in the broader-scale climate datasets (Guisan *et al*., 2007), such as the WorldClim (Fick and Hijmans, 2017) or Chelsa climate datasets (Karger *et al*., 2017). Broader-scale climate datasets may have resulted in bias model predictions especially in mountainous areas. This study developed a practical and applicable method to generate high-resolution climate dataset for modeling species distribution in mountainous areas. The statistical method developed in this study had generated two high-resolution climate datasets from two data sources. RF method based on these two high-resolution climate datasets had successfully projected potential distribution range of natural grassland in mountainous areas.

High-resolution climate dataset can improve model performance only when it had successfully reflected heterogeneous climate features in mountainous areas. In NTWN, remarkably steep precipitation gradient from coastal to inland areas was evidently caused by winter monsoon. High-resolution climate dataset derived from the meteorological data, the AdjMCD50, had successfully

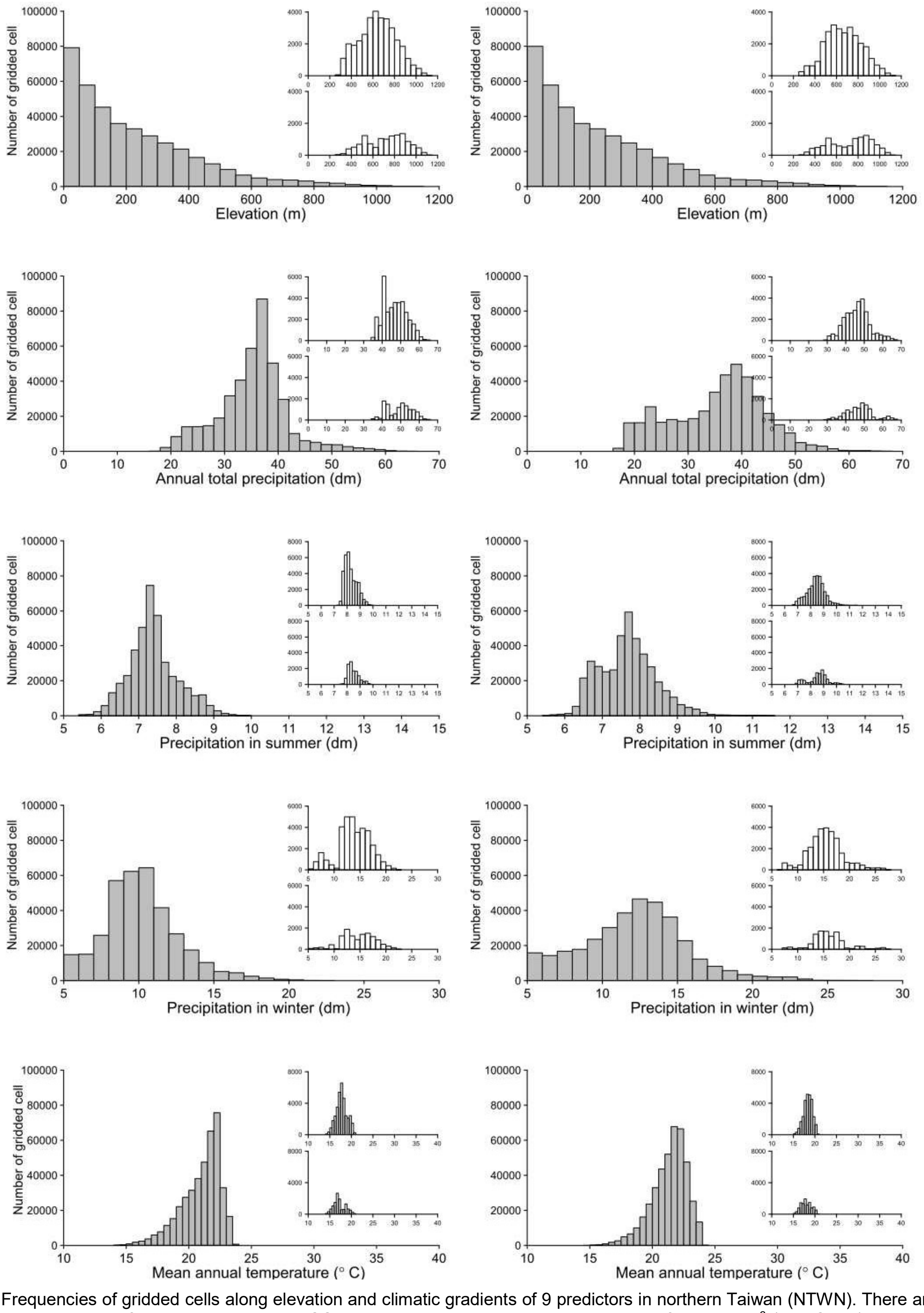

Fig. 6. Frequencies of gridded cells along elevation and climatic gradients of 9 predictors in northern Taiwan (NTWN). There are two climate datasets, the left column is adjusted TCCIP climate dataset with spatial resolution of 50 × 50 m^2 (AdjTCD50) and the right column is adjusted meteorological climate dataset with spatial resolution of 50 × 50 m^2 (AdjMCD50). The grey histograms present the frequency of total gridded cells in the NTWN. The subplot with white histograms present the frequency of gridded cells with presence of natural grassland projected by Random Forests based on pseudo-absence data (upper subplot) and true absence data (lower subplots). TCCIP is the Taiwan Climate Change Projection Information and Adaptation Knowledge Platform.

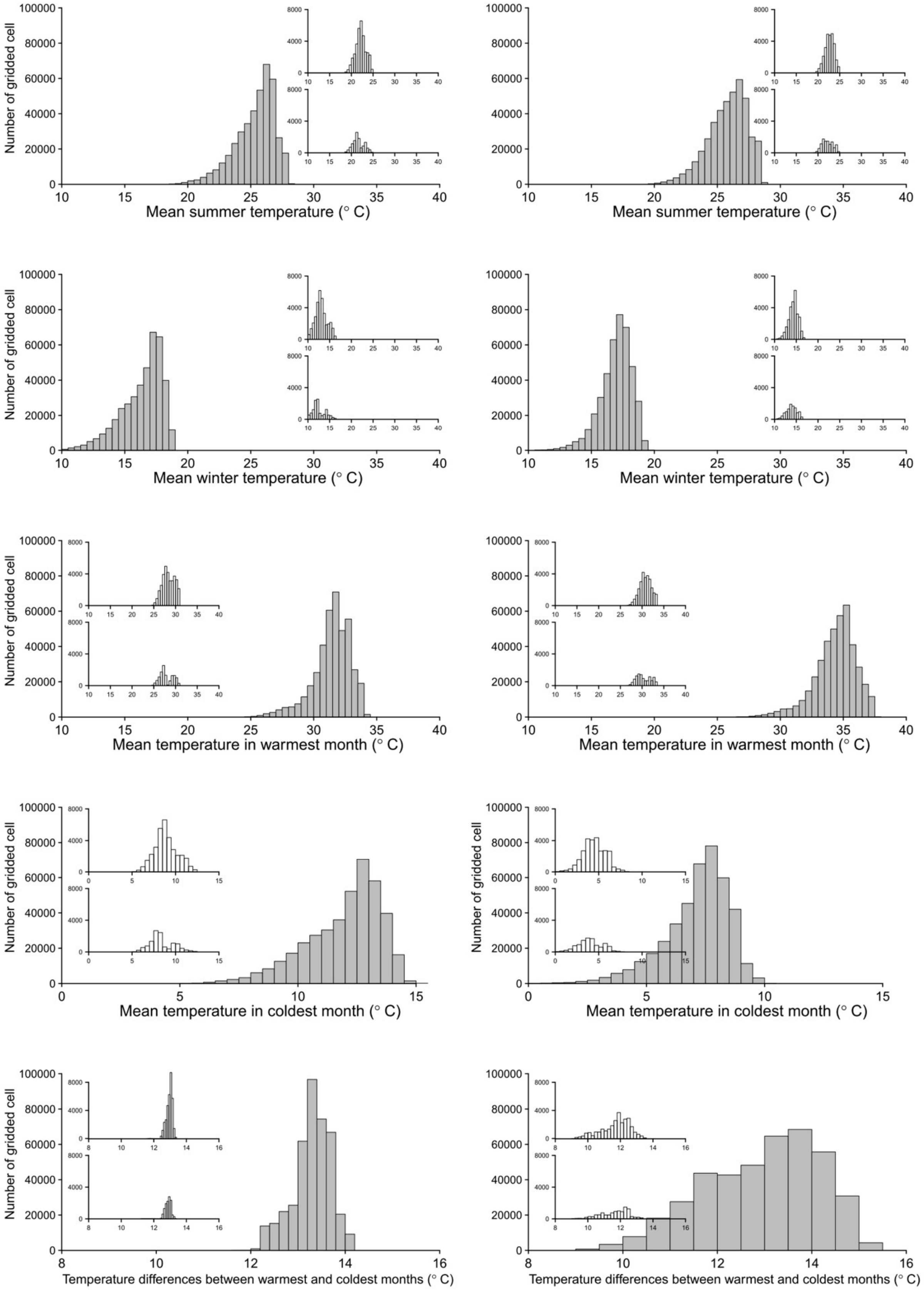

Fig. 6. Continued.

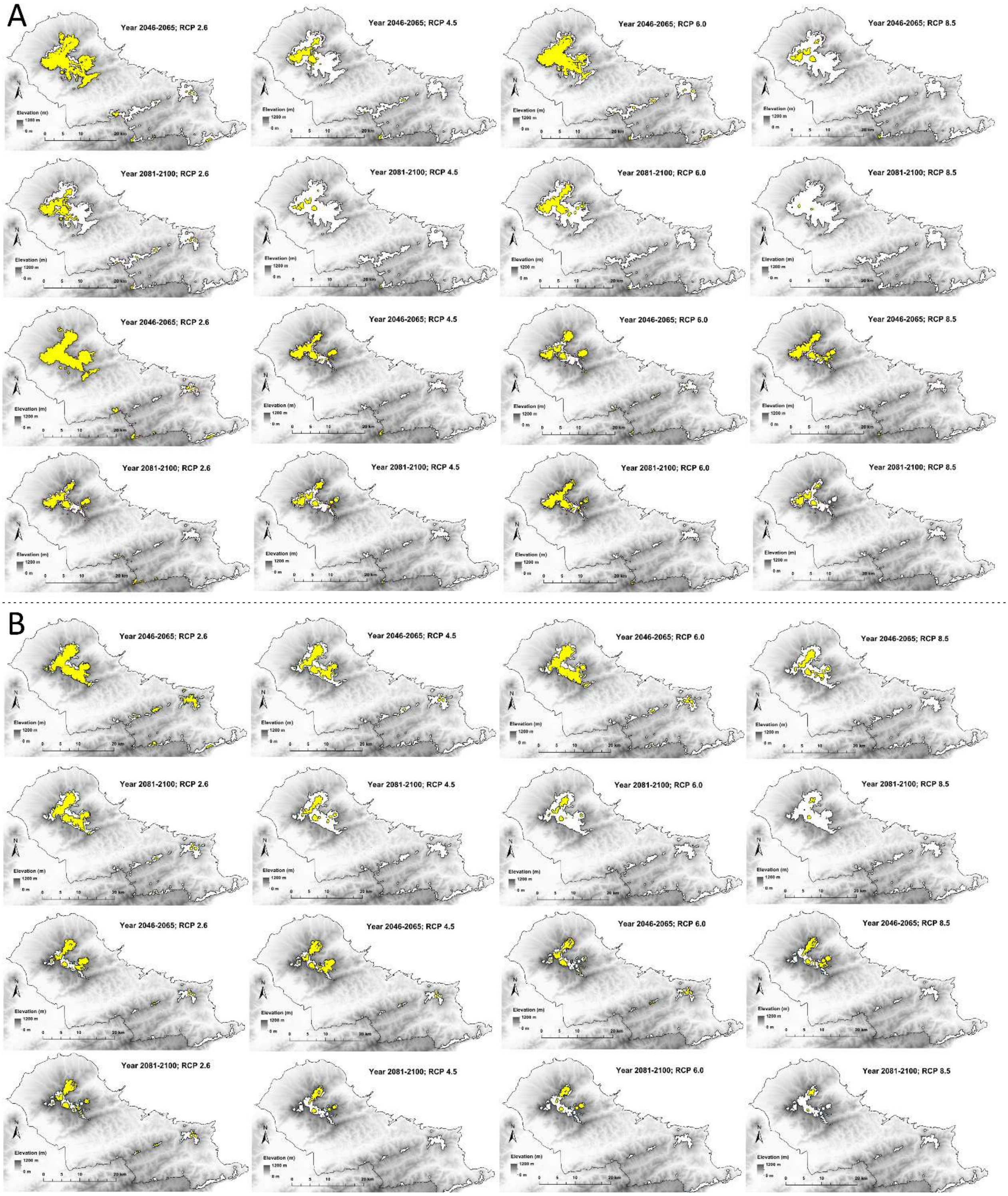

Fig 7. Suitable habitats of natural grassland under climate change projected by Random Forests (RF) based on (**A**) adjusted TCCIP climate dataset with 50 × 50 m^2 spatial resolution (AdjTCD50) and (**B**) based on adjusted meteorological climate dataset with 50 × 50 m^2 spatial resolution (AdjMCD50). The white area with dark outline is the historical distribution range based on pseudo-absence (upper two rows of A and B) and true absence data (lower two rows of A and B). The yellow areas are future distribution ranges projected by RF based on the future climate datasets at mid (2046-2065) and late (2081-2100) of the 21th century that were derived from TCCIP climate dataset and adding changing amounts of the four climate scenarios. The four columns present distribution ranges of natural grassland under RCP 2.6 (left column), 4.5 (mid left column), 6.0 (mid right column), and 8.5 (right column). The future climate projections of Taiwan island were downscaled from the CESM1-CAM5. TCCIP is the Taiwan Climate Change Projection Information and Adaptation Knowledge Platform..

captured this steep precipitation gradient as well as highly heterogeneous climate features in NTWN (Fig. 3B). On the contrary, the AdjTCD50 derived from the TCCIP gridded climate dataset presented a precipitation gradient from low to high elevations (Fig. 3A). Although the AdjTCD50 and AdjMCD50 reflected distinct precipitation gradients, they presented similar pattern of annual mean temperature along mountain slopes in NTWN (Fig. 3B and 3D). In addition, distinct precipitation gradients were not the only differences between the AdjTCD50 and ADjMCD50. The frequencies of gridded cells along the gradients of Tcld, Twrm, and Tdif were different between the AdjTCD50 and ADjMCD50 climate datasets. The two climate datasets presented different climate conditions of NTWN. Given the circumstance, meteorological data is the practical and direct records of climate conditions in mountainous areas. High-resolution climate dataset derived from direct and practical data records is available to reflect heterogeneous climate features in mountainous areas. In contrast, TCCIP gridded climate dataset downscaled from GCMs was indirect climate data source that had generated more gentle and more even climatic conditions in mountainous areas. The distinct climate features of the two high-resolution climate datasets were apparently caused by different data sources but not the procedure of the statistical method.

Even though the precipitation gradients presented by AdjTCD50 and AdjMCD50 were distinct in NTWN, RF method based on these two climate datasets projected similar distribution ranges of natural grassland along mountain ridge in the study area. Prediction distribution range based on the AdjMCD50 was distantly more close to the true absence data of natural grassland. True absence data was geographically close to the real boundaries of natural grassland in NTWN, so the model results close to the true absence data had more precisely projected the distribution range of natural grassland. In spite of this result, model prediction based on the AdjTCD50 was not an error performance, it was merely not as accurate as that based on the AdjMCD50. Thus, model performance based on the high-resolution climate datasets derived from coarser one, such as TCCIP gridded climate dataset, or derived from meteorological data were both useful for model predictions. Meteorological data is a better source to generate high-resolution climate dataset for SDMs in mountainous areas. However, meteorological station is usually sparse in mountainous areas which makes the coarser gridded climate dataset the only available data source of mountainous areas. If coarser gridded climate dataset is the only available data source, the method developed in this study is still applicable to interpolate high-resolution climate dataset in mountainous areas and model results based on the derived high-resolution climate dataset are potentially acceptable.

Meteorological data is certainly a better source to generate high-resolution climate dataset for capturing climate heterogeneity in mountainous areas. However, meteorological data do not present future climate scenarios. Therefore, high-resolution future climate datasets were necessary to generate from gridded climate datasets derived from GCMs. This study also developed a novel method to generate high-resolution future climate datasets for various warming conditions. The relative changes of the mid and late of the 21th century to the early 21th century climate data were added to the high-resolution climate datasets to generate future climate projections in the study area. The high-resolution future climate datasets were available to project restricted distribution range of natural grassland at the mid and end of the 21th century (Fig. 7). The statistical method to generate high-resolution future climate datasets is practically useful for RF method to project range shifts of plant species and is recommended to apply for some other mountainous areas.

Occurrences of natural grassland along mountain ridges at low elevation is consistent with the presence of low elevation treeline in NTWN. Treeline was characterized by harsh environments, such as cold soil temperature (Korner, 1998; Liu *et al*., 2011; Smith *et al*., 2009). Lowest temperature in coldest month was proposed to be the probable factor associated with the occurrence of low elevation treeline in NTWN (Liao and Chen, 2022). Temperature plays as a critical factor to limit growth of tree species in NTWN and may have related to the potential distribution range of natural grassland. In this study, the temperature factor presented similar pattern along mountain slopes between the two climate datasets had resulted in similar potential distribution range of natural grassland predicted by RF. In addition, increases of temperatures at the mid and end of this century have evidently caused distributional constraints of natural grassland as well as potential expansion of the evergreen broadleaved forests in NTWN. Future climate dataset generated in this study are supposedly useful for projecting future geographical range shifts of ecosystems in mountainous areas.

In this study, natural grassland was played as a target vegetation for evaluating the expansion or constraint of distribution range. Distinct boundaries between natural grassland and evergreen broadleaved forests make the natural grassland as a good target for model predictions. Model results determined that natural grassland in NTWN is susceptible to climate change and distribution range of natural grassland will be constraint at the end of the 21th century. Also, rare species depend on the ecosystem of natural grassland are likely to be threatened by constraint of natural grassland under climate change. Impacts of climate change on the species distribution range in mountainous areas deserve particular conservation attentions, since these species are likely to react sensitively to climate change.

In NTWN, *Miscanthus sinensis* and *Pseudosasa usawai* are the predominant species of natural grassland along mountain ridges (Liao *et al*., 2014). It is a critical issue that climatic niches of these two species are indiscriminate and are probably having convergent climatic niche in mountainous areas. Niche convergence of phylogenetic distantly related species was proposed to be a primary role in driving community assembly in local vegetation (Pearse and Hipp, 2012; Qian, 2017). Further studies will be necessary to conduct on this topic in NTWN to identify characteristics of climatic niches between these two species and to evaluate their responses to climate change.

The values of TSS and ROC were both higher while RF was applied by pseudo-absence data (Fig. 5). The TSS is indicator of discrimination capacity, which quantifies how well the model can distinguish presences from absences or vice versa (Hao *et al*., 2019). On the other hand, ROC curve illustrates the performance of a classifier across the entire range of a decision threshold (Khoshgoftaar *et al*., 2007). Pseudo-absence points environmentally distant from the presence points increase the rate of well-predicted absence (Lobo *et al*., 2008) and evidently decrease the omission and commission errors of model predictions. On the contrary, true absence data were geographically and environmentally close to the presence points that increases omission and commission errors of model predictions. Pseudo-absence data geographically distant from the presence points caused higher values of the TSS and ROC index. Despite of, model predictions were still recommended to apply by true absence data because true absence data had accurately delineated the geographical distribution ranges and environmental spaces of plants.

Habitat fragmentation and steep climatic gradient are common features in mountainous areas because of complex topography. Native mountainous species are usually habitat-restricted and are more vulnerable to climate change. Particularly, rare species with locally restrict distribution are often critically affected by certain local elements, such as the occurrences of favorable microsites and microclimates (Elith and Leathwick, 2009; Heikkinen *et al*., 2012). Thus, designation of effective protected areas for conserving plant species is a challenging task in mountains areas and it relies on an accurate distribution map to show geographical extent and favorable microsites in mountainous areas. However, management planning often suffers from a lack of accurate distribution map, resulting in a poor understanding of species biogeographical patterns and ecological requirements (Lannuzel *et al*., 2021). An accurate distribution map projected by SDMs relies on a high resolution climate dataset. High-resolution climate dataset precisely captured heterogeneous climate features in mountainous areas are expected to project accurate distribution maps of plant species showing geographical extent in mountain areas. High-resolution climate datasets generated in this study had evidently improved model performance and provides effective information on conservation management in response to climate change. The statistical method developed in this study is confidently applied to generate high-resolution historical and future climate datasets. Most importantly, the statistical method is available to interpolate high-resolution climate dataset even from coarser gridded climate dataset. Model predictions based on the high-resolution climate datasets may have better expressed the climatic requirements and exact climatic niches of species and may provide useful suggestions for designation of conservation management in mountainous areas.

ACKNOWLEDGMENTS

The authors want to thank for Mr. Shi-Chieh Kuo and some students in the Department of Life Science, Chinese Culture University, Taipei, Taiwan for their helps in data collections. The authors appreciate Mr. Kai-Jie Yang in the Institution of Geography, Chinese Culture University, Taipei, Taiwan for technical support of ArcGIS software. This work was in part supported by Yangmingshan National Park, Construction and Planning Agency Ministry of the Interior, Executive Yuan, Taipei, Taiwan. The authors are also thankful to Taiwan Climate Change Projection Information and Adaptation Knowledge Platform for data providing and financial sponsor.

LITERATURE CITED

Allen, C. D., Macalady, A. K., Chenchouni, H., Bachelet, D., McDowell, N., Vennetier, M., Kitzberger, T., Rigling, A., Breshears, D.D., Hogg, E.H., Gonzalez, P., Fensham, R., Zhang, Z., Castro, J., Demidova, N., Lim, J.-H., Allard, G., Running, S.W., Semerci, A., Cobb, N. 2010. A global overview of drought and heat-induced tree mortality reveals emerging climate change risks for forests. For. Ecol. Manag. **259(4)**: 660–684.

Ashcroft, M. B., Gollan, J. R. 2012. Fine-resolution (25 m) topoclimatic grids of near-surface (5 cm) extreme temperatures and humidities across various habitats in a large (200× 300 km) and diverse region. Int. J. Climatol. **32(14)**: 2134–2148.

Ashcroft, M. B., Gollan, J. R., Warton, D. I., Ramp, D. 2012. A novel approach to quantify and locate potential microrefugia using topoclimate, climate stability, and isolation from the matrix. Glob. Change Biol. **18(6)**: 1866–1879.

Boulesteix, A. L., Janitza, S., Kruppa, J., König, I. R. 2012. Overview of random forest methodology and practical guidance with emphasis on computational biology and bioinformatics. Wiley Interdiscip. Rev.: Data Min. Knowl. Discov. **2(6)**: 493–507.

Breiman, L. 2001. Random forests. Mach. Learn. **45(1)**: 5–32.

Chambers, J., Hastie, T. 1992. Linear models. Chapter 4 of statistical models in S. Wadsworth & Brooks/Cole.

Chen, W. K., Tsai, C. Y. 1983. The climate of Yangmingshan National Park. Yangmingshan National Park, Construction and Planning Agency Ministry of the Interior, Executive Yuan, Taipei, Taiwan.

Chiou, C.R., Song, G.Z.M., Chien, J.H., Hsieh, C.F., Wang, J.-C., Chen, M.Y., Liu, H.Y., Yeh, C.L., Hsia, Y.J., Chen, T.Y. 2010. Altitudinal distribution patterns of plant species in Taiwan are mainly determined by the northeast monsoon rather than the heat retention mechanism of Massenerhebung. Bot. Stud. **51(1)**: 89–97.

Dingman, J. R., Sweet, L. C., McCullough, I., Davis, F. W., Flint, A., Franklin, J., Flint, L. E. 2013. Cross-scale modeling of surface temperature and tree seedling establishment in mountain landscapes. Ecol. Process. **2(1)**: 1–15.

Dobrowski, S.Z. 2011. A climatic basis for microrefugia: the influence of terrain on climate. Glob. Change Biol. **17(2)**: 1022–1035.

Elith, J., Leathwick, J.R. 2009. Species distribution models: ecological explanation and prediction across space and time. Annu. Rev. Ecol. Evol. Syst. **40(1)**: 677–697.

Evans, J.S., Cushman, S.A. 2009. Gradient modeling of conifer species using random forests. Landsc. Ecol. **24(5)**: 673–683.

Fatemi, S. S., Rahimi, M., Tarkesh, M., Ravanbakhsh, H. 2018. Predicting the impacts of climate change on the distribution of *Juniperus excelsa* M. Bieb. in the central and eastern Alborz Mountains, Iran. iForest **11(5)**: 643–650.

Fick, S. E., Hijmans, R. J. 2017. WorldClim 2: new 1-km spatial resolution climate surfaces for global land areas. Int. J. Climatol. **37(12)**: 4302–4315.

Fois, M., Fenu, G., Lombrana, A. C., Cogoni, D., Bacchetta, G. 2015. A practical method to speed up the discovery of unknown populations using Species Distribution Models. J. Nat. Conserv. **24:** 42–48.

Fridley, J. D. 2009. Downscaling climate over complex terrain: high finescale (< 1000 m) spatial variation of near-ground temperatures in a montane forested landscape (Great Smoky Mountains). J. Appl. Meteorol. Climatol. **48(5)**: 1033–1049.

Godsoe, W., Murray, R., Plank, M. J. 2015. Information on biotic interactions improves transferability of distribution models. Am. Nat. **185(2)**: 281–290.

Greiser, C., Meineri, E., Luoto, M., Ehrlén, J., Hylander, K. 2018. Monthly microclimate models in a managed boreal forest landscape. Agric. For. Meteorol. **250**: 147–158.

Guisan, A., Zimmermann, N.E., Elith, J., Graham, C.H., Phillips, S., Peterson, A.T. 2007. What matters for predicting the occurrences of trees: techniques, data, or species characteristics? Ecol. Monogr. **77(4)**: 615–630.

Hamann, A., Wang, T. 2006. Potential effects of climate change on ecosystem and tree species distribution in British Columbia. Ecology **87(11):** 2773–2786.

Hao, T., Elith, J., Guillera-Arroita, G., Lahoz-Monfort, J. J. J. D., Distributions. 2019. A review of evidence about use and performance of species distribution modelling ensembles like BIOMOD. **25(5)**: 839–852.

Heikkinen, R. K., Marmion, M., Luoto, M. 2012. Does the interpolation accuracy of species distribution models come at the expense of transferability? Ecography **35(3)**: 276–288.

Hsieh, C. F., Chao, W. C., Liao, C. C., Yang, K. C., Hsieh, T. H. 1997. Floristic composition of the evergreen broad-leaved forests of Taiwan. Nat. Hist. Res. **4**, 1–16.

Hu, X.-G., Wang, T., Liu, S.-S., Jiao, S.-Q., Jia, K.-H., Zhou, S.-S., Jin, Y., Li, Y., El-Kassaby, Y.A., Mao, J.-F. 2017. Predicting future seed sourcing of *Platycladus orientalis* (L.) for future climates using climate niche models. Forests **8(12)**: 471.

IPCC. 2013. The Physical Science Basis. Contribution of Working Group I to the Fifth Assessment Report of the Intergovernmental Panel on Climate Change Cambridge University Press, Cambridge, United Kingdom and New York, NY, USA.

Iturbide, M., Bedia, J., Gutiérrez, J. M. 2018. Background sampling and transferability of species distribution model ensembles under climate change. Glob. Planet. Change **166:** 19–29.

Karger, D. N., Conrad, O., Böhner, J., Kawohl, T., Kreft, H., Soria-Auza, R. W., Zimmermann, N.E., Linder, H.P., Kessler, M. 2017. Climatologies at high resolution for the earth's land surface areas. Sci. Data **4(1)**: 170122.

Kay, J. E., Deser, C., Phillips, A., Mai, A., Hannay, C., Strand, G., Arblaster, J. M., Bates, S. C., Danabasoglu, G., Edwards, J., Holland, M., Kushner, P., Lamarque, J.-F., Lawrence, D., Lindsay, K., Middleton, A., Munoz, E., Neale, R., Oleson, K., Polvani, L., Vertenstein, M. 2015. The Community Earth System Model (CESM) large ensemble project: A community resource for studying climate change in the presence of internal climate variability. Bull. Am. Meteorol. Soc. **96(8)**: 1333–1349.

Keppel, G., Van Niel, K. P., Wardell-Johnson, G. W., Yates, C. J., Byrne, M., Mucina, L., Schut, A.G.T., Hopper, S.D., Franklin, S.E. 2012. Refugia: identifying and understanding safe havens for biodiversity under climate change. Glob. Ecol. Biogeogr. **21(4)**: 393–404.

Khoshgoftaar, T. M., Golawala, M., Van Hulse, J. 2007. An empirical study of learning from imbalanced data using random forest. 19th IEEE International Conference on Tools with Artificial Intelligence **(ICTAI 2007)**: 310–317.

Korner, C. 1998. A re-assessment of high elevation treeline positions and their explanation. Oecologia **115(4)**: 445–459.

Korner, C., Paulsen, J. 2004. A world-wide study of high altitude treeline temperatures. J. Biogeogr. **31(5)**: 713–732.

Lannuzel, G., Balmot, J., Dubos, N., Thibault, M., Fogliani, B. 2021. High-resolution topographic variables accurately predict the distribution of rare plant species for conservation area selection in a narrow-endemism hotspot in New Caledonia. Biodivers. Conserv. **30(4)**: 963–990.

Lenoir, J., Hattab, T., Pierre, G. 2017. Climatic microrefugia under anthropogenic climate change: implications for species redistribution. Ecography **40(2)**: 253–266.

Li, C. F., Chytrý, M., Zelený, D., Chen, M. Y., Chen, T. Y., Chiou, C. R., Hsia, Y.-J., Liu, H.-Y., Yang, S.-Z., Yeh, C.-L., Wang, J.-C., Yu, C.-F., Lai, Y.-J., Chao, W.-C., Hsieh, C.-F., Bruelheide, H. 2013. Classification of Taiwan forest vegetation. Appl. Veg. Sci. **16(4)**: 698–719.

Liao, C. C., Chang, C. R., Hsu, M. T., Poo, W. K. 2014. Experimental evaluation of the sustainability of dwarf bamboo (*Pseudosasa usawai*) sprout-harvesting practices in Yangminshan National Park, Taiwan. Environ. Manage. **54(2)**: 320–330.

Liao, C. C., Chen, Y. H. 2021. Improving performance of species distribution model in mountainous areas with complex topography. Ecol. Res. 36(4): 648–662.

Liao, C.C., Chen, Y.H. 2022. The effects of true and pseudo-absence data on the performance of species distribution models at landscape scale. Taiwania **67(1)**: 9–20.

Liao, C.C., Kuo, S.C., Chang, C.R. 2012. Forest distribution on small isolated hills and implications on woody plant distribution under threats of global warming. Taiwania **57(3)**: 242–250.

Liaw, A., Wiener, M. 2002. Classification and regression by random. Forest. R news **2(3)**: 18–22.

Lin, H. Y., Hu, J. M., Chen, T. Y., Hsieh, C. F., Wang, G., Wang, T. 2018. A dynamic downscaling approach to generate scale-free regional climate data in Taiwan. Taiwania **63(3)**: 251–266.

Lin, H. Y., Li, C. F., Chen, T. Y., Hsieh, C. F., Wang, G., Wang, T., Hu, J. M. 2020. Climate-based approach for modeling the distribution of montane forest vegetation in Taiwan. Appl. Veg. Sci. **23(2)**: 239–253.

Lin, L.-Y., Lin, C.-T., Chen, Y.-M., Cheng, C.-T., Li, H.-C., Chen, W.-B. 2022. The Taiwan Climate Change Projection Information and Adaptation Knowledge Platform: A decade of climate research. Water **14(3)**: 358.

Liu, B., Liang, E., Zhu, L. 2011. Microclimatic conditions for *Juniperus saltuaria* treeline in the Sygera Mountain, Southeastern Tibetan Plateau. Mt. Res. Dev. **31(1):** 45–53.

Lobo, J. M., Jiménez-Valverde, A., Real, R. 2008. AUC: a misleading measure of the performance of predictive distribution models. Glob. Ecol. Biogeogr. **17(2)**: 145–151.

Maria, B., Udo, S. 2017. Why input matters: Selection of climate data sets for modelling the potential distribution of a treeline species in the Himalayan region. Ecol. Modell. **359**, 92–102.

Meineri, E., Hylander, K. 2017. Fine-grain, large-domain climate models based on climate station and comprehensive topographic information improve microrefugia detection. Ecography **40(8)**: 1003–1013.

Mi, C., Huettmann, F., Guo, Y., Han, X., Wen, L. 2017. Why choose Random Forest to predict rare species distribution with few samples in large undersampled areas? Three Asian crane species models provide supporting evidence. PeerJ, **5**, e2849.

Miles, L., Grainger, A., Phillips, O. 2004. The impact of global climate change on tropical forest biodiversity in Amazonia. Glob. Ecol. Biogeogr. **13(6)**: 553–565.

Mohapatra, J., Singh, C.P., Hamid, M., Verma, A., Semwal, S.C., Gajmer, B., Khuroo, A.A., Kumar, A., Nautiyal, M.C., Sharma, N., Pandya, H.A. 2019. Modelling *Betula utilis* distribution in response to climate-warming scenarios in Hindu-Kush Himalaya using random forest. Biodivers. Conserv. **28(8-9)**: 2295–2317.

Orsenigo, S., Montagnani, C., Fenu, G., Gargano, D., Peruzzi, L., Abeli, T., Alessandrini, A., Bacchetta, G., Bartolucci, F., Bovio, M., Brullo, C., Brullo, S., Carta, A., Castello, M., Cogoni, D., Conti, F., Domina, G., Foggi, B., Gennai, M., Gigante, D., Iberite, M., Lasen, C., Magrini, S., Perrino, E.V., Prosser, F., Santangelo, A., Selvaggi, A., Stinca, A., Vagge, I., Villani, M., Wagensommer, R.P., Wilhalm, T., Tartaglini, N., Duprè, E., Blasi, C., Rossi, G. 2018. Red Listing plants under full national responsibility: extinction risk and threats in the vascular flora endemic to Italy. Biol. Conserv. **224**: 213–222.

Pearse, I.S., Hipp, A.L. 2012. Global patterns of leaf defenses in oak species. Evolution **66(7)**: 2272–2286.

Qian, H. 2017. Climatic correlates of phylogenetic relatedness of woody angiosperms in forest communities along a tropical elevational gradient in South America. J. Plant Ecol. **11(3)**: 394–400.

Qiao, H., Feng, X., Escobar, L. E., Peterson, A. T., Soberón, J., Zhu, G., Papeş, M. 2019. An evaluation of transferability of ecological niche models. Ecography **42(3)**: 521–534.

Schorr, G., Holstein, N., Pearman, P., Guisan, A., Kadereit, J. 2012. Integrating species distribution models (SDMs) and phylogeography for two species of Alpine *Primula*. Ecol. Evol. **2(6)**: 1260–1277.

Smith, W. K., Germino, M. J., Johnson, D. M., Reinhardt, K. 2009. The altitude of alpine treeline: A Bellwether of climate change effects. Bot. Rev. **75(2):** 163–190.

Su, H. J. 1984. Studies on the climate and vegetation types of the natural forests in Taiwan (II) Altitudinal vegetation zones in relation to temperature gradient. Quarterly Journal of Chinese Forestry **17**: 57–73.

Thomas, C. D., Cameron, A., Green, R. E., Bakkenes, M., Beaumont, L. J., Collingham, Y. C., Erasmus, B.F.N., de Siqueira, M.F., Grainger, A., Hannah, L., Hughes, L., Huntley, B., van Jaarsveld, A.S., Midgley, G.F., Miles, L., Ortega-Huerta, M.A., Peterson, A. T., Phillips, O.L., Williams, S. E. 2004. Extinction risk from climate change. Nature **427(6970)**: 145–148.

Thuiller, W., Georges, D., Engler, R., Breiner, F., Georges, M. D., Thuiller, C. W. 2016. Package 'biomod2'. Species distribution modeling within an ensemble forecasting framework.

Vanneste, T., Michelsen, O., Graae, B. J., Kyrkjeeide, M. O., Holien, H., Hassel, K., Lindmo, S., Kapás, R.E., De Frenne, P. 2017. Impact of climate change on alpine vegetation of mountain summits in Norway. Ecol. Res. **32(4):** 579–593.

Vanwalleghem, T., Meentemeyer, R. 2009. Predicting forest microclimate in heterogeneous landscapes. Ecosystems **12(7)**: 1158–1172.

Walther, G.-R. 2010. Community and ecosystem responses to recent climate change. Philos. Trans. R. Soc. Lond. B Biol Sci. **365(1549)**: 2019–2024.

Wang, T., Hamann, A., Spittlehouse, D., Carroll, C. 2016. Locally downscaled and spatially customizable climate data for historical and future periods for North America. PLoS One **11(6)**: e0156720.

Weng, S., Yang, C. 2012. The construction of monthly rainfall and temperature datasets with 1km gridded resolution over Taiwan area (1960–2009) and its application to climate projection in the near future (2015–2039). Atmos. Sci. **40(4)**: 349–369.

Williams, J. N., Seo, C., Thorne, J., Nelson, J. K., Erwin, S., O'Brien, J. M., Schwartz, M. W. 2009. Using species distribution models to predict new occurrences for rare plants. Divers. Distrib. **15(4):** 565–576.

Xu, Y., Huang, Y., Zhao, H., Yang, M., Zhuang, Y., Ye, X. 2021. Modelling the effects of climate change on the distribution of endangered *Cypripedium japonicum* in China. Forests **12(4)**: 429.

Zhao, X., Meng, H., Wang, W., Yan, B. 2016. Prediction of the distribution of alpine tree species under climate change scenarios: *Larix chinensis* in Taibai Mountain (China). Pol. J. Ecol. **64(2)**: 200–212.

Zhu, Y., Wei, W., Li, H., Wang, B., Yang, X., Liu, Y. 2018. Modelling the potential distribution and shifts of three varieties of *Stipa tianschanica* in the eastern Eurasian Steppe under multiple climate change scenarios. Glob. Ecol. Conserv. **16**: e00501.

Supplementary materials are available from Journal Website